Available online at www.sciencedirect.com
ScienceDirect
Chemical Physics Letters 452 (2008) 188–192
CHEMICAL PHYSICS LETTERS
www.elsevier.com/locate/cplett

Surface effect of nano-phosphors studied by time-resolved spectroscopy of Ce^{3+}

L.J. Tian [a,b,c], Y.J. Sun [a,c], Y. Yu [a], X.G. Kong [a,*], H. Zhang [c,*]

[a] Key Laboratory of Excited State Process, Changchun Institute of Optics, Fine Mechanics and Physics, Chinese Academy of Sciences, Changchun 130033, PR China
[b] Graduate School of Chinese Academy of Sciences, Beijing 100039, PR China
[c] Van't Hoff Institute for Molecular Sciences, University of Amsterdam, Nieuwe Achtergracht 166, 1018 WV Amsterdam, The Netherlands

Received 5 October 2007; in final form 20 December 2007
Available online 31 December 2007

Abstract

Surface effects on nanoparticles have been explored by picosecond time-resolved spectroscopy using Ce^{3+} ions doped in yttrium aluminum garnet (YAG) nano-phosphors (NPS) as a probe. Non-exponential decays have been observed over the entire emission band that could be fitted well with four decay components varying from ~150 ps to ~70 ns. These components have been assigned to originate from sites different in distance from the surface. Surface quenching effects have been found to be negligible when the luminescence centers are more than 7 nm away from the surface.

1. Introduction

The surface states of nanoparticles have been studied extensively in recent years since they are responsible for many superior properties of nanoparticles which have led to their application in various fields, such as lighting and cathode ray tubes, as well as in biology and medicine [1–6]. In nano-phosphors (NPS) the surface states are formed by: (i) the non-radiative relaxation centers due to the surface defects which are comprised of dangling bonds in the grain-boundary and of defects caused by the distorted crystal lattice on the surface [7,8]; (ii) organic groups such as hydroxyl, carboxylate, etc. stuck to the surface [9]. There is no doubt that understanding how the surface states affect the optical property of NPS is crucial in view of optimizing their emission properties and the surface coating/modification for further use in many fields, especially in biology [10]. However, despite the efforts to unravel the mechanism, our understanding of the surface is still limited compared with the application needs.

Rare earth ions have been regarded as an ideal probe for the study of the surface structure of the nanoparticles, e.g. Eu^{3+} [11–14]. This is because the typical magnetic dipole transition of $^5D_0 \rightarrow {}^7F_1$ of Eu^{3+} ions is sensitive to the local environment. It has been confirmed that the lower symmetry of the surface lattice induces broadening in the luminescence spectra of Eu^{3+} in YVO_4 [6], and that organic solvents and/or ligands quench the luminescence of Eu^{3+} in LaF or $LaPO_4$ as well [15]. These results gave an intuitive picture on how quenching occurs by the surface quenching centers or the high energy vibration modes of the OH^- and carboxylate anions.

In this Letter we have employed time-resolved spectroscopic techniques to study the surface influence on the NPS using Ce^{3+} ions as a probe. Compared with Eu^{3+}, Ce^{3+} has several advantages in time-resolved spectroscopic studies: (i) it has only one electron in the rather simple ground state, which facilitates analysis; (ii) the emission is due to the electric dipole parity-allowed 5d→4f transition that is not shielded by the outer electronic shell and the

* Corresponding authors. Fax: +31 20 525 5604 (H. Zhang).
E-mail addresses: xgkong14@ciomp.ac.cn (X.G. Kong), h.zhang@uva.nl (H. Zhang).

0009-2614/$ - see front matter © 2007 Elsevier B.V. All rights reserved.
doi:10.1016/j.cplett.2007.12.058

energy splitting is therefore more sensitive to the local crystal field; (iii) the lifetime (ns) is much shorter than that of Eu^{3+}, which facilitates full time range measurements. Previously, steady-state fluorescence spectra of Ce^{3+} – doped nanoparticles had been reported, that were claimed to be similar to the spectra of their bulk counterpart [16]. In this Letter we have analyzed the emission of Ce^{3+} doped in YAG over the full time range. The emission from Ce^{3+} occupied in various sites from interior to surface layers has been distinguished. The similarity of steady-state spectra of Ce^{3+} in the nanoparticle and in the bulk counterpart is explained. Our study verifies that the surface states only influence the Ce^{3+} in the sites less than 7 nm from the surface.

2. Experimental

YAG: Ce^{3+} nanoparticles were prepared by modified polyacrylamide-gel methods [17], the molar concentration of Ce^{3+} was 1.67 mol%. The gel was dried in an oven at 80 °C, and then sintered at 900 °C for 2 h with a temperature rising rate of 2 °C/min. To identify the crystallization phase and determine the mean size of crystallites, X-ray diffraction (XRD) analysis was carried out with a powder diffractometer (Rigaku, D/max rA), using Cu Kα radiation ($\lambda = 0.154$ nm). The microstructures of the samples were studied using a scanning electron microscopy (JSM6301F). IR spectra were measured on a BioRad FT–IR (FTS-7) spectrophotometer. The steady-state florescence spectra were measured on a Spex Fluorolog 3 spectrofluorometer (Jobin-Yvon) equipped with a solid powder sample holder. Time-resolved florescence was acquired using the time correlated single photon counting (TCSPC) technique (IRF ~ 17 ps) in time windows of 5 and 100 ns. The TCSPC setup has been described elsewhere [18]. Excitation light (460 nm) was generated by frequency-doubling of the 920 nm Coherent Chameleon laser and the instrument response is ~17 ps. To acquire luminescence decay on an even longer time scale, an oscilloscope was employed in combination with photomultiplier detection and excitation by a Coherent Infinity-XPO laser (460 nm, laser pulse width 2.75 ns, 10 Hz repetition rate).

3. Results and discussion

Fig. 1a shows the XRD pattern of YAG:Ce^{3+}, which indicates that the pure cubic YAG phase (JCPDS File No. 79-1891) was formed without other structures such as Y_2O_3, Al_2O_3, YAP, YAM, etc. The average size of the sample was 37 nm as obtained from the XRD by applying Scherer equation to the full width at half maximum of the (420) diffraction peak, which is consistent with the result based on SEM images of more than 100 nano-particles (see Fig. 2b). In the FTIR spectrum (Fig. 1c) the broad absorption bands at 1650 cm^{-1} and 3500 cm^{-1} derive from OH^- groups adsorbed on the surface of the NPS, while the

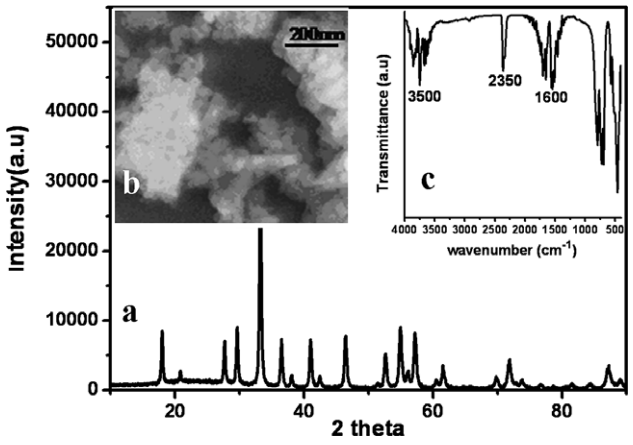

Fig. 1. X-ray powder diffraction patterns (a), SEM image (b) and FT–IR spectrum (c) of 1.67 mol% Ce^{3+} doped YAG nanocrystals, prepared by sol–gel method.

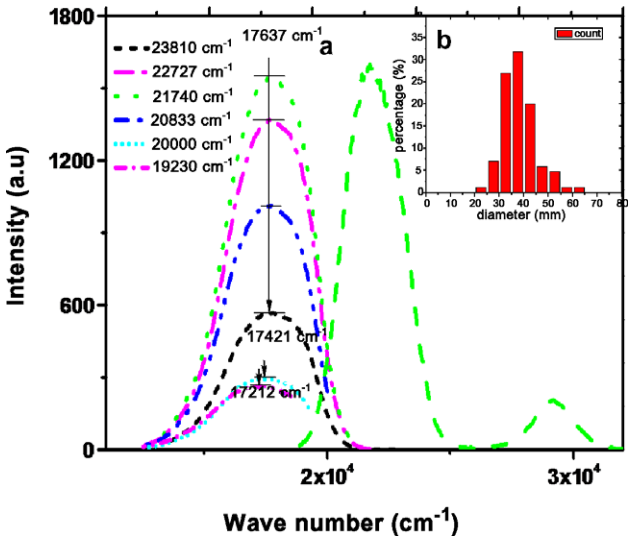

Fig. 2. (a) PL spectra (left) with different excitation wavenumbers and PLE spectrum (right). All fluorescence spectra are measured at room temperature and calibrated. (b) Histogram of the particle size distributions obtained from SEM images of more than 100 nano-particles.

peaks around 1500 cm^{-1} and 2350 cm^{-1} belong to the carboxylate anion and residual CO_2, respectively [19].

Excitation and emission spectra are shown in Fig. 2a. The broad emission band is attributed to the lowest-lying 5d to 4f transition of the Ce^{3+} ion. We notice that the line width of the emission spectrum of NPS is broader than that of Ce^{3+} in bulk materials, which is ascribed to the inhomogeneous broadening in NPS [8–10]. For NPS, the Ce^{3+} ions experience different crystal fields because of an imperfect and/or distorted crystalline lattice predominantly caused by the surface. The different environments broaden the emission spectrum of Ce^{3+} ions in NPS. Selective excitation, being performed from 19230 cm^{-1} to 23810 cm^{-1} as shown in Fig. 2a clearly shows that when the excitation energy decreases the emission peaks shift to red. Such a broadening and shift can be attributed to the co-existence

of multiple fluorescent centers that are all excited by photons with energy higher than 21 740 cm^{-1}. From this picture it is also readily deduced that the lifetimes of various luminescent centers should be different, since they experience different surroundings.

In view of these results, luminescence decay traces have been obtained. Representative luminescence decay curves in windows of 1 μs, 100 ns, and 5 ns are depicted in Fig. 3a–d, respectively, under 460 nm laser excitation. It is obvious that the decay curves are multi-exponential. For bulk YAG:Ce^{3+}, the Ce^{3+} ions occupy exclusively the dodecahedral Y^{3+} site, and the lifetime is typically 65 ns in a single crystal or in ceramic materials [11,12]. Recently it was reported that the decay curves of cerium ions in YAG bulk materials are either mono-exponential or bi-exponential with a long tail [20]. In our case, the decay curves show a non-exponential behavior even in a 5 ns time window. It was found that at least four exponential components were needed to come to an acceptable fit of the data, i.e.

$$I(\lambda, t) = \sum_{i=1}^{4} A_i(\lambda) * \exp\left(-\frac{t}{\tau_i}\right) \quad (1)$$

In which τ_i and $A_i(\lambda)$ are the lifetime and amplitude of the *i*th type of luminescence centers, respectively. After de-convolution of the data with the response function of the TCSPC setup decay times of 150 ps, 1.75 ns, 14.5 ns and 70 ns were obtained. The 150 ps and 70 ns components were obtained by fitting the decay curves in the 5 ns and 1 μs time windows, respectively.

Mechanisms responsible for a multi-exponential decay in principle can include multi-sites, concentration quenching, surface defects, etc. As aforementioned, only one site for the yttrium ions in YAG is substituted by Ce^{3+} ions. It is also known that the host-associated defects of YAG are F or F^{+} centers as well as the Y_{Al} anti-site defects [21,22], which emit around 340 nm – out of the luminescence band of Ce^{3+}. Since the amount of dopant-induced defects has been found to be much less in the interior than in the surface layer in NPS [23], the interior defects were neglected in our analysis.

It has also been proposed that concentration quenching might lead to multi-exponential decay [24]. However, the quenching concentration of the rare earth ions is much higher in the nano-system than in the bulk counterpart [25–27]. The quenching concentration of YAG:Ce^{3+} nano-crystal synthesized by sol–gel synthetic method is higher than 4% [28,29]. Hence, the quenching process is not expected to happen in the present case where the dopant concentration is only 1.67%. Furthermore, the longest component is found to be comparable to that in the bulk material, being in conflict with the concentration mechanism in which the long lifetime should be shorter than the intrinsic lifetime of the activator. Setlur and Srivastava have discussed this issue in bulk material [30]. Although the

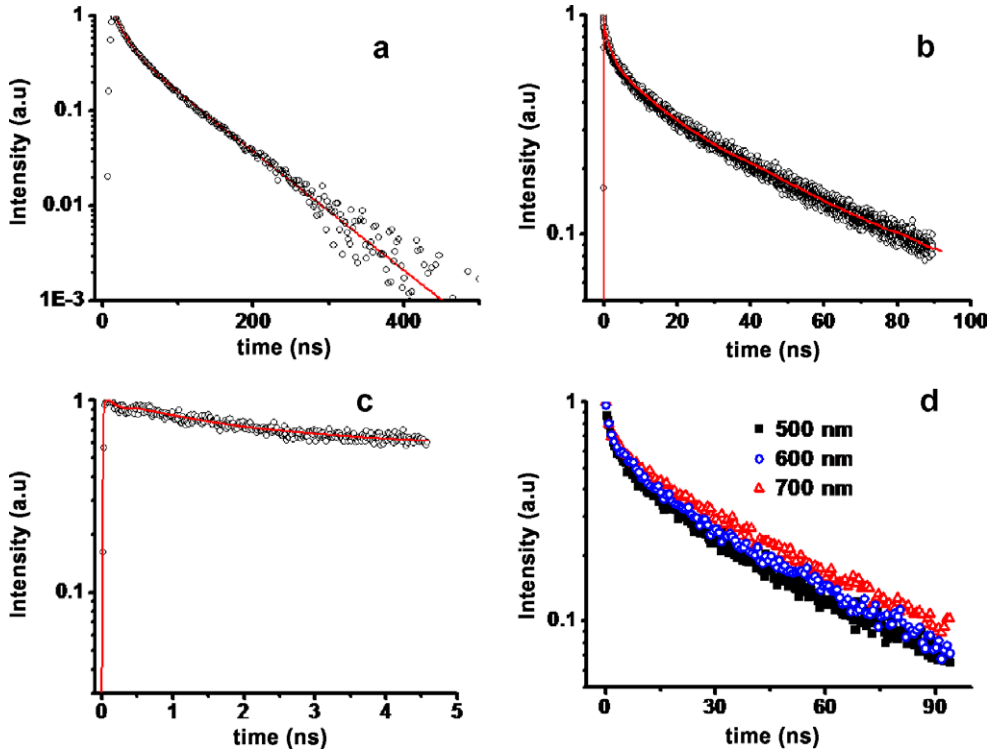

Fig. 3. Luminescence decay curves at 550 nm of Ce^{3+} doped in YAG in different time windows: (a) 1 μs, (b) 100 ns, (c) 5 ns. The decay curves measured at different wavelengths in 100 ns window are given in (d).

1.67% concentration is somewhat higher than the critical energy transfer concentration of 1.2% in YAG:Ce^{3+} bulk material, no build-up component in the luminescence traces has been found in our experiments, which indicates that the quenching concentration of the Ce^{3+} ions is higher in NPS.

Homogeneous distribution of Ce^{3+} in YAG nanosystem is expected because of the high similarity in size, charge and reactivity of the lanthanide ions. Besides, sol–gel synthetic approach has been proven to be an effective way of preparing nanocrystals with homogeneous dopant distribution, which was evidenced by high resolution electron microscopy coupled EDX analysis where the doped samples exhibited no heterogeneity with respect to the distribution of cerium [29,31,32].

The multi-exponential decay is therefore primarily attributed to the surface states, which may act as quenching centers because of the larger surface-to-volume ratio of NPS. In order to get further insight into the surface effects, we have constructed the initial spectra ($t = 0$) for each component normalized to the steady-state PL spectrum (Fig. 4a). As is shown in the figure, the spectra of shorter components are blue-shifted compared to that of the longest one. In the surface layer of the NPS, the relevant crystal field has lower symmetry and is weaker than in the interior resulting in a smaller splitting of the 5d band [33]. As a result, the energy difference between the lowest energy level of 5d and 4f ground level is larger. The spectra of the Ce^{3+} ions closer to surface should thus be blue-shifted compared to those located further inside the nanoparticle. Moreover, it is noted that the emission intensities of 150 ps, 1.75 ns, 14.5 ns and 70 ns components are almost equal. If we make the hypothesis that the transition moments of all the Ce^{3+} ions are similar, the amplitudes of each of the four components would be proportional to the numbers of each type of Ce^{3+}. In this way, a simplified model can be established in relation with the surface effect as illustrated in Fig. 4b, where the Ce^{3+} ions are distributed homogeneously in the lattice sphere. The longest lifetime is attributed to ions in the core of the NPS, while the shorter components derive from ions in the outer three shells. From this model it can be readily deduced that the thickness of the surface layer where the quenching takes place, is about 7 nm. Previously, it has been determined that the critical energy transfer distance between Ce^{3+} in YAG and an energy acceptor on the surface of the nanoparticle is also about 7 nm [34]. Our results are therefore in excellent agreement with this assignment.

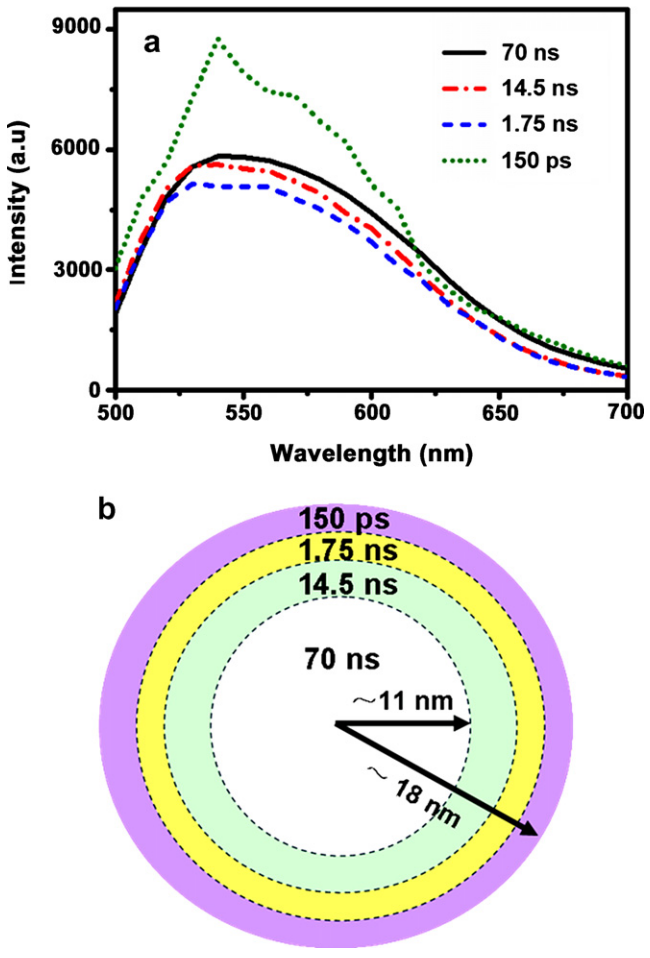

Fig. 4. (a) PL spectra of the four components at $t = 0$ and (b) a simplified conceptual model based on the time-resolved spectroscopic results.

As the quenching of the excited Ce^{3+} ions by the surface quenching centers occurs via a dipole–dipole mechanism, the quenching rate should follow R^{-6} relation [15]. The excited state depopulation rate of the Ce^{3+} ions is described by the following equation:

$$W_{\tau_i} = W_R + W_{NR}(R), \quad \tau_i = 1/W_{t_i} \tag{2}$$

where W_R and W_{NR} represent the radiative and non-radiative transition rate, respectively. W_{NR} is proportional to R^{-6} and rather sensitive to the R, and the lifetime τ_i of Ce^{3+} ions at a different distance from the surface to the core in the NPS can be distinctly different. It is expected that quenching is more severe when the Ce^{3+} ions are closer to the surface of the particles, i.e., when R becomes smaller. An additional source of quenching could derive from the organic functional groups, introduced during the chemical synthesis, which may stick to the surface. These groups may accelerate the quenching process because of high-energy vibrational modes associated with O–H and C=O, which existed even when the sample was sintered at 900 °C (Fig. 1c). This could explain that the luminescence was heavily quenched as evidenced by the shortening of the lifetime to 150 ps in our sample.

We would like, however, to stress that the model in which the dopant distribution is divided into four components is just a simplified concept of real continuous situation.

Finally, we would like to comment on the observation that the steady-state spectrum of Ce^{3+} ions doped in NPS is similar to that of their bulk counterpart. As the steady-state spectrum is simply a time integration of the emission decay, the steady-state spectrum would be domi-

nated by the longest lifetime component since the relevant amplitudes are similar (vide supra). From our aforementioned discussion it is clear that the longest component is from the Ce^{3+} ions located in the core where the energy transfer to the quenching centers is negligible and their spectrum should be similar to the one doped in bulk material. Therefore it is reasonable that the steady-state spectrum of Ce^{3+} in nanosystem does not differ much from their bulk counterpart.

4. Conclusions

In summary, Ce^{3+} luminescence in YAG nano-phosphors has demonstrated a non-exponential decay behavior, which is ascribed to the quenching by the surface states. Employing time-resolved spectroscopic techniques, four representative quenching regimes have been brought in as a simplified approach to the real continuous situation. The closer the Ce^{3+} ions approach the surface, the more severe the quenching and the faster the luminescence decay. When the Ce^{3+} ions are located further into the nanoparticle, say >7 nm from the surface, the quenching effect is negligible and the spectrum behaves like its bulk counterpart.

Acknowledgments

This work was supported by NSFC of China, National (863) Project, and exchange program between CAS of China and KNAW of the Netherlands. Technical support of Dick Bebelaar and John van Ramesdonk is highly appreciated. We thank Fred Brouwer and Wybren Jan Buma for valuable suggestions.

References

[1] B.M. Tissue, Chem. Mater. 10 (1998) 2837.
[2] Z.G. Wei, L.D. Sun, C.S. Liao, C.H. Yan, Appl. Phys. Lett. 80 (2002) 1447.
[3] P. Zhang, S. Rogelj, K. Nguyen, D. Wheeler, J. Am. Chem. Soc. 128 (2006) 12410.
[4] S.F. Lim, R. Riehn, W.S. Ryu, N. Khanarian, C. Tung, D. Tank, R.H. Austin, Nano Letters 6 (2006) 169.
[5] J.C. Boyer, F. Vetrone, J.A. Capobianco, A. Speghigi, M. Bettinelli, J. Phys. Chem. B 108 (2004) 20137.
[6] C.H. Yan, L.D. Sun, C.S. Liao, Y.X. Zhang, Y.Q. Lu, S.H. Huang, S.Z. Lu, Appl. Phys. Lett. 82 (2003) 20.
[7] W.D. Kingery, J. Am. Ceram. Soc. 57 (1974) 1.
[8] E. Zych, C. Brecher, J. Glodo, J. Phys.: Condens. Matter 12 (2000) 1947.
[9] G. Xiong, U. Palb, J. Garcia Serrano, J. Appl. Phys. 101 (2007) 024317.
[10] P. Zhang, W. Steelant, M. Kumar, M. Scholfield, J. Am. Chem. Soc. 129 (2007) 4526.
[11] V. Sudarsan, F.C.J.M. van Veggel, R.A. Herring, M. Raudsepp, J. Mater. Chem. 15 (2005) 1332.
[12] J.J. Chang, S. Xiong, H.S. Peng, L.D. Sun, S.Z. Lu, F.T. You, S.H. Huang, J. Lumin. 122–123 (2007) 844.
[13] P. Ghosh, S. Sadhu, A. Patra, Phys. Chem. Chem. Phys. 8 (2006) 3342.
[14] Y.J. Sun, Y. Chen, L.J. Tian, Y. Yu, X.G. Kong, J.W. Zhao, H. Zhang, J. Lumin. 128 (2008) 15.
[15] J.W. Stouwdam, G.A. Hebbink, J. Huskens, F.C.J.M. van Veggel, Chem. Mater. 15 (2003) 4604.
[16] C.H. Lu, H.C. Hong, R. Jagannathan, J. Mater. Chem. 12 (2002) 2525.
[17] Q. Li, L. Gao, D.S. Yan, Mater. Chem. Phys. 64 (2000) 41.
[18] D. Bebelaar, Rev. Sci. Instrum. 57 (1986) 6.
[19] L. Vien, The Handbook of IR and Raman Characteristic Frequencies of Organic Molecules, Academic Press, NY, 1991.
[20] E. Zych, C. Brecher, J. Glodo, J. Phys.: Condens. Matter. 12 (2000) 1947.
[21] C.L. Wang, D. Solodovnikov, K.G. Lynn, Phys. Rev. B 73 (2006) 233204.
[22] E. Zych, C. Brecher, H. Lingertat, J. Lumin. 78 (1998) 121.
[23] V. Sudarsan, F.C.J.M. van Veggel, R.A. Herring, M. Raudsep, J. Mater. Chem. 15 (2005) 1332.
[24] R. Balda, J. Fernandez, M.A. Arriandiaga, L.M. Lacha, J.M. Fernandez-Navarro, Opt. Mater. 28 (2006) 1253.
[25] W.P. Zhang et al., Chem. Phys. Lett. 292 (1998) 133.
[26] C. Jia, L. Sun, F. Luo, X. Jiang, L. Wei, C. Yan, Appl. Phys. Lett. 84 (2004) 5305.
[27] Z. Wei, L. Sun, C. Liao, C. Yan, Appl. Phys. Lett. 80 (2002) 1447.
[28] Y.X. Pan, M. M Wu, Q. Su, J. Phys. Chem. S. 65 (2004) 845.
[29] A. Katelnikovas, P.K. Vitta, P. Pobedinskas, G. Tamulaitis, A.Z. ukauskas, J.E. J gensen, A. Kareiva, J. Cryst. Growth 304 (2007) 361.
[30] A.A. Setlur, A.M. Srivastava, Opt. Mater. 29 (2007) 1647.
[31] G.D. Xia, S.M. Zhou, J.J. Zhang, J. Xu, J. Cryst. Growth 279 (2005) 357.
[32] M. Veith, S. Mathur, A. Kareiva, M. Jilavi, M. Zimmera, V. Huch, J. Mater. Chem. 9 (1999) 3069.
[33] P. Dorenbos, J. Lumin. 99 (2002) 283.
[34] S.F. Wuister, C.D.M. Donega, A. Merjerink, Phys. Chem. Chem. Phys. 6 (2004) 1633.